

A Mössbauer experiment on Mars

E. Kankeleit, J. Foh, P. Held, G. Klingelhöfer and R. Teucher

*Institut für Kernphysik, Technical University of Darmstadt,
Schlossgartenstrasse 9, D-64289 Darmstadt, Germany*

A Mössbauer spectrometer for the mineralogical analysis of the Mars surface is under development. This instrument will be installed on a Mars-Rover, which is part of the Russian Mars'96 mission. Due to power and mass restrictions, the electromechanical drive and the electronic components have been extremely miniaturized, and for the rude conditions during take-off and landing, very much ruggedized in comparison to standard systems. Solid-state detectors (PIN-diodes) are used for γ - and X-ray detection in backward geometry and will also give information on the elemental composition by X-ray fluorescence spectroscopy. The different operations of the spectrometer are controlled autonomously by a microprocessor.

1. Introduction

In the coming decades, the iron oxide red planet Mars will play an essential part in the study of the solar system by spacecraft missions. There are plans at the space centers NASA (United States of America), ESA (Europe), and IKI (Russia) to install stationary and mobile systems on the surface of Mars. Part of the scientific payload of the Russian Mars-96 mission [1] is a ^{57}Fe Mössbauer (MB) spectrometer installed on a rover of about 1 m in size, to be placed on the surface of Mars [15,16]. Such a spectrometer is also being developed for the US planetary program [13,14].

The elemental composition of Martian soil was determined by X-ray fluorescence analysis during the Viking mission in 1976 [2], but not its mineralogical composition. One suggestion is that it is composed mainly of iron-rich clay minerals, with an iron content of about $14(\pm 2)$ wt.%. The soil also contains about 5 wt.% of a strongly magnetic mineral, perhaps maghemite ($\gamma\text{-Fe}_2\text{O}_3$) [2]. In addition to other elements, about $0.6(\pm 0.2)\%$ of Ti was found by X-ray fluorescence. It will be significant to establish whether the magnetic phase on the surface of Mars contains titanium or not. The pathways of formation of maghemite and titanomaghemite are very different [7,8]. Also of extreme interest is the oxidation state of the iron and the mineral composition of the Mars surface. To both questions, MB spectroscopy can provide important information. The question "Why do an MB experiment on Mars?" has been extensively discussed by Knudsen at the last ICAME conference [5–7]. Here, we will try to give an answer to the question "How does one do an MB experiment on Mars?"

The big step forward in having a rover compared to the stationary Viking lander is the possibility to study different samples at different geologically attractive places. For the MB setup, it will be of importance to take spectra from the fine soil on the surface, from rocks, and from the deepest few centimeters of the soil, which may be accessible by using a digging wheel of the rover or possibly by a drilling device.

For the Mars-96 mission, the small rover of overall size of 1 m and weight of approximately 70 kg will supply a total of 10–13 W electric power on average. Only a fraction of this power will be allotted for experiments. The total weight for the approximately eight experiments will be limited to only 10–15% of the weight of the rover.

The MB experiment will be positioned together with an α -backscattering experiment [37] and a small TV camera on a robotic arm.

As mentioned above, the Martian soil contains a significant amount of a magnetic material. It would be desirable to also have the possibility of magnetic separation, which would allow this component to be identified with high accuracy. The use of permanent magnets as on the Viking mission [2], or maybe of a magnet array as now included in the US MESUR Pathfinder mission [21, 22], in combination with the MB instrument will allow this. This proposal [9] is now seriously considered for the Mars-96 mission.

The experiments have to withstand accelerations over a broad bandwidth in frequency up to 200 g, as well as the large diurnal temperature variations on the Martian surface. The memory and transputer chips have to survive two years of cosmic ray irradiation. According to the COSPAR requirements (less than 300 spores per m² [10]), sterilizing procedures are necessary before departure and have to be considered in the construction. Fortunately, these fall into a category less stringent than for the Viking mission.

Of great importance is the ambient temperature, which will be between 180 K and 290 K during a Martian day at equatorial landing sites. There is no power left for temperature control but, as will be shown below, this is of great advantage for both the detectors and the samples, which may then be investigated over a range of measurable temperatures.

Another problem is the microphonics due to other experiments, the rover itself or, in particular, to winds or even dust storms expected in the Martian autumn. This makes a sturdy connection between sample and MB drive essential. For these reasons, the pickup voltage from the drive will be used as a check for the level of microphonics before the start of the MB experiment.

Because of the dusty atmosphere, the MB system has to be airtight and precautions to avoid a dust-covered entrance window have to be taken.

Due to restrictions in data transfer (20 minutes Mars–Earth travel time; low rover–orbiter transfer rate), the MB system has to boot with an “on” command and the data have to be stored within the system and wait for contact between rover and orbiter.

The measuring times for a particular sample have to be of the order of a few hours depending on the rover program. Because of the expected complex spectra over a large dynamic range in velocity, high detection efficiency is extremely important. How we hope to achieve this will be discussed in the following.

2. Method

As shown above, sample preparation as needed for a transmission experiment must be excluded. However, the MB backscattering technique is highly suitable for a rover mission with the possibility of selecting samples. This was already recognized in an early proposal for this mission [3].

The main disadvantage of backscattering is the secondary radiation caused by the 122 keV transition. For a reduction of the background at 14.4 keV and the 6.4 keV X-ray line, good energy resolution of the detector system is required, but also high count-rate capabilities with the strong sources to be used. Good resolution is even more important for elemental analysis with the X-ray fluorescence technique. For this reason, Si-PIN diodes were chosen as detectors instead of a set of gas counters, considered in [4,39].

The general setup of our “Miniaturized Mössbauer backscattering Spectrometer” (MIMOS) is shown in fig. 1.

3. Experimental setup

The system has the size of a soft drink can, a weight less than 500 g, and a power consumption of less than 3 W. The ^{57}Co source is mounted on the small drive and surrounded by a graded shield. Collimated radiation passes through a Be window and the reemitted radiation is detected by a ring-like array of PIN diodes behind the same Be window. For noise reduction and high count rate, there are six independent preamplifier–amplifier–ADC channels. Data storage and data transfer is controlled by a transputer, which also produces the velocity reference signal. There is a seventh channel for velocity calibration of the MB drive, with a small source mounted on the top of the drive and a reference absorber in transmission geometry (see fig. 1). In addition, there is a temperature sensor active during the MB experiment, and during the off time, vibrations will be detected.

Some of the parts of the system will now be discussed in more detail.

3.1. MÖSSBAUER SOURCE AND SHIELDING

The highest possible source strength is desirable; however, the source has to be sized to fit the given system. This dictates the specific activity, which is limited by the requirement that over a period of two years the natural linewidth should not increase by more than a factor of 2–3. Calculations indicate an optimum

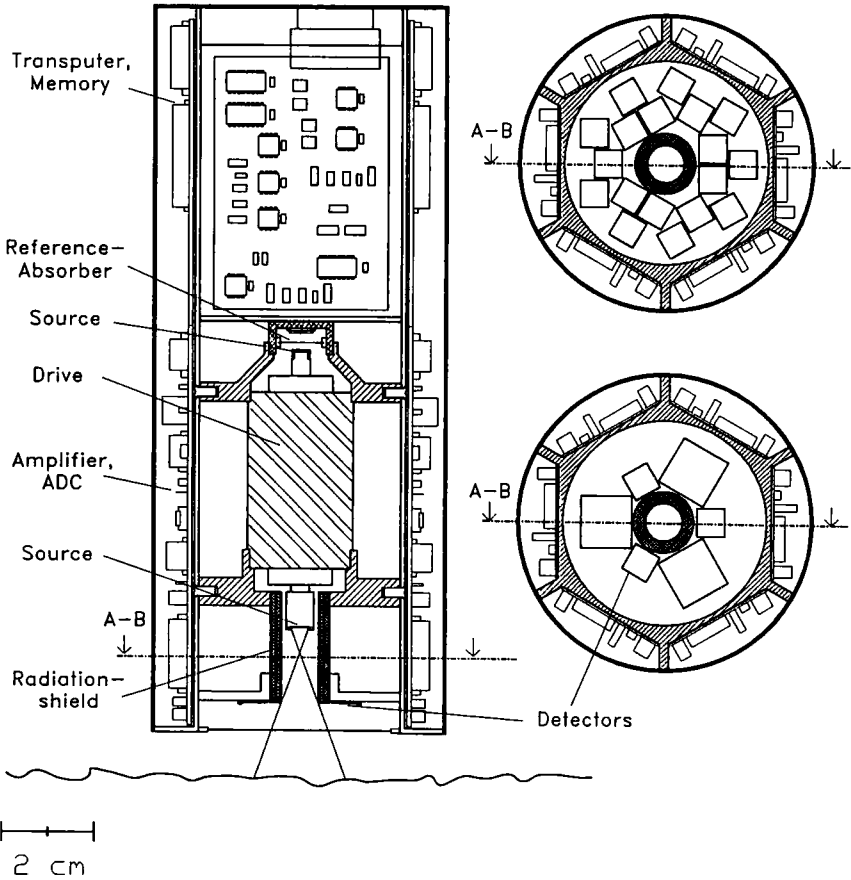


Fig. 1. Mössbauer spectrometer MIMOS for backscattering geometry with two possible detector arrangements, as seen from the bottom.

at 1 Ci/cm^2 [17–19]. Sources of $150 \text{ mCi } ^{57}\text{Co}$ in Rh with this specific activity and of comparable quality to commercial sources were supplied by IKI. With the rhodium matrix, no additional broadening due to the low temperatures on Mars should occur.

Most important is an effective shielding of the PIN diodes from direct and cascade radiation. The 8 mm inner diameter graded shield consists of concentric tubes of 0.5 mm thick brass, 1 mm U, 1 mm W and another 0.5 mm brass. No 122 keV radiation is seen in the detectors. This shielding acts also as a collimator, limiting the maximum emission angle to 25° and reducing the cosine smearing [42] to a level that still allows a reasonable separation of the outer lines of γ - and α - Fe_2O_3 .

3.2. DRIVE SYSTEM

The simplest way to fulfil the space and weight conditions was to scale down the drive system we have been building at this institute [11, 12]. A decisive aspect in this scaling is the size and the mass (2–4 g) of the sources and we thus constructed a drive about one fifth the size of our standard system. This has a diameter of 22 mm, a length of 40 mm, and about 50 g mass.

The system with the SmCo permanent magnets was newly optimized with regard to a homogeneous and high magnetic field in the coil gap. For this, an elaborate computer code (at the Gesellschaft für Schwerionenforschung (GSI)) was used and good agreement between calculations and experimental results, using a Hall sensor, were found.

The decisive improvements of the drive, made during the last decades, are a rigid tube connection between the driving and the velocity pickup coils in the double-loudspeaker arrangement, and good shielding between the two coils to avoid cross talk. The short tube guarantees a fast transfer of information with the velocity of sound in the aluminum, and thus a minimum phase lag and a high feedback gain margin. Fortunately, despite the increase of unwanted cross talk due to the smaller distance between the coils, the relative contribution is still less than 0.01% in the frequency domain of the triangular wave form and is thus tolerable.

These relations are depicted in fig. 2 in the Bode diagram of the transfer function, which is the output voltage over input current as a function of frequency. The $1/f$ behavior above the main resonance at about 25 Hz extends up to 20 kHz. The small dipole at about 2 kHz is of no relevance for the feedback behavior. The available gain at the point of -180° phase determines the possible feedback gain of 3×10^3 , which is excellent. Because of the steep phase change at this point, additional filtering makes no sense and was not used. The figure also shows the calculated transfer function for an Al tube having the speed of sound of 5000 m/s. The first resonance of the tube shows up at $1/T = c/l = 25$ kHz (see fig. 2). This is in reasonable agreement with the experimental results considering the rather complex structure of the tube. Due to the shorter tube, this drive achieves a feedback gain and performance in triangular velocity motion superior to our standard drive. For the light weight sources, the linearity is better in comparison to the standard drive, and the difference signal is nearly free of ringing.

The drive will be running at about 25 Hz frequency, at which is also has its main resonance. This low frequency allows a broad bandwidth for the closed-loop system and good performance with triangular reference signal. However, this is asking for rather soft springs. As a consequence, a rotation of the drive from horizontal to vertical position in earth gravity leads to a shift of the tube of about 0.4 mm. The resulting nonlinearity between velocity and pickup voltage is still tolerable within the 0.1% accuracy. In principle, this can be compensated by a dc current. On Mars, with a factor 3 smaller gravity forces, this will create no problem and no correction is needed.

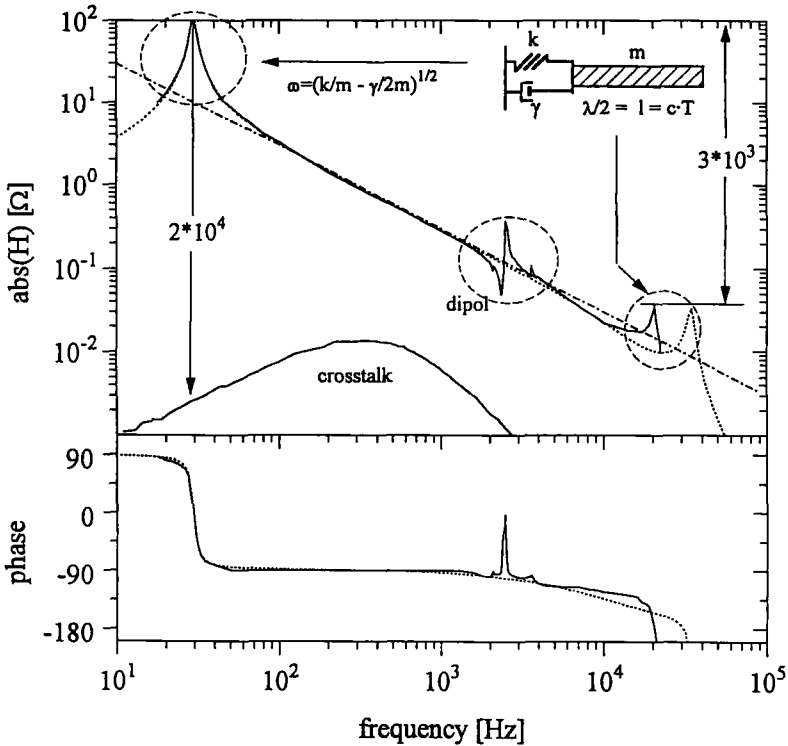


Fig. 2. Amplitude $\text{abs}(H)$ and phase transfer function of the drive as a function of frequency of the input current. $\text{Abs}(H)$ is the ratio of the output voltage of the pickup coil and the input current of the driving coil. The phase is given in degrees. Also indicated is the cross talk and the calculated transfer behavior for an Al tube (dashed line).

The whole system, including the drive, has to survive a brutal testing procedure, which will be performed partly in Toulouse, France [45]. Concerning the large accelerations during launch and landing, the construction provides limiters to avoid the destruction of the soft Kapton springs.

Velocity calibration and control of linearity will be done by recording simultaneously a calibration spectrum using a second source at the other end of the moving tube. A combination of reference absorbers is considered, as for instance $\alpha\text{-Fe}$, $\gamma\text{-}$ or $\alpha\text{-Fe}_2\text{O}_3$, both magnetically split, and the quadrupole split SNP ($\text{Na}_2[\text{Fe}(\text{CN})_2\text{NO}]2\text{H}_2\text{O}$). From the temperature dependence of the hyperfine interaction, an average temperature can be deduced.

3.3. DETECTOR SYSTEM AND ELECTRONICS

For a backscatter geometry, a detector system covering a large solid angle is needed to minimize data acquisition time. Because the secondary radiation created

by the 122 keV γ -rays creates background in the 14.4 keV and the 6.4 keV window, good energy resolution of the detector is desirable such that a narrow window set on these lines will produce a good signal-to-background ratio.

The detector system consists of silicon PIN diodes [36] with a $5 \times 5 \text{ mm}^2$ or $10 \times 10 \text{ mm}^2$ active area in an array arrangement as indicated in the two options in fig. 1. A thickness of about 400 μm is a good choice according to our experience. The efficiencies for the 6.4 and 14.4 keV radiation are nearly 100% and about 65%, respectively. Diodes with a greater thickness and therefore higher efficiency for the 14.4 keV radiation, having a smaller capacity at diminishing leakage current, available as unmounted chips, and selected for low noise and acceptable prices are still requested.

As mentioned above, the temperatures on Mars are well below freezing point. Fortunately, the energy resolution improves at lower temperatures [20]. Figure 3 shows the energy spectra for two temperatures. In fig. 4, the temperature dependence of the resolution and the leakage current is depicted for two different detector sizes. The leakage current is the dominant source for the line broadening at higher temperatures. The improved resolution of the smaller diode originates from its lower capacity.

Spectra of $^{57}\text{Co}/\text{Rh}$ radiation backscattered from an Al and a stainless steel (SS) plate, which are equal in recording time, are shown in fig. 5. A continuum is seen above 122 keV, resulting from the few 692 keV γ quanta which are not completely absorbed in the shielding. No photo peak appears at 122 keV. However, this radiation shows up in a broad Compton distribution, being more intense for the lower Z Al. A second Compton distribution originates in the detector itself, as seen in the rising slope starting below 40 keV. On top of these, we see a peak at the 22.1 keV due to the Ag backing of the detector. Below that in SS at zero velocity, the 14.4 keV MB resonance line and also the 6.4 keV X-ray line dominate, whereas in Al only the 14.4–0.4 keV Compton scattered line appears.

The good energy resolution, in particular during the cold Martian night (see above and fig. 4), makes an X-ray fluorescence measurement for elemental analysis – especially for higher Z – feasible. One of the amplifier branches for a small HgI_2 detector is being considered for use, which gives the best resolution even at room temperature [37,38]. As mentioned above, for the interpretation of the MB spectra it is important to resolve the Ti X-rays of 4.51 keV [6].

A high energy resolution is required for each of the diodes. Therefore, the noise contributions have to be minimized. This means each of the detectors needs its own preamplifier–amplifier–ADC system (see fig. 1 and fig. 6). A 12-bit ADC, selected for good differential linearity, is used. Only the most significant 8 bits are read out. Therefore, no sliding-scale technique is required. Two digital windows at 6.4 keV and 14.4 keV are set by the transputer software. Two single-channel discriminators set at these energies would also do the job, but this would not decrease the number of chips. In addition, the performance of the system has to be checked many times again, and this is most easily done by taking energy spectra.

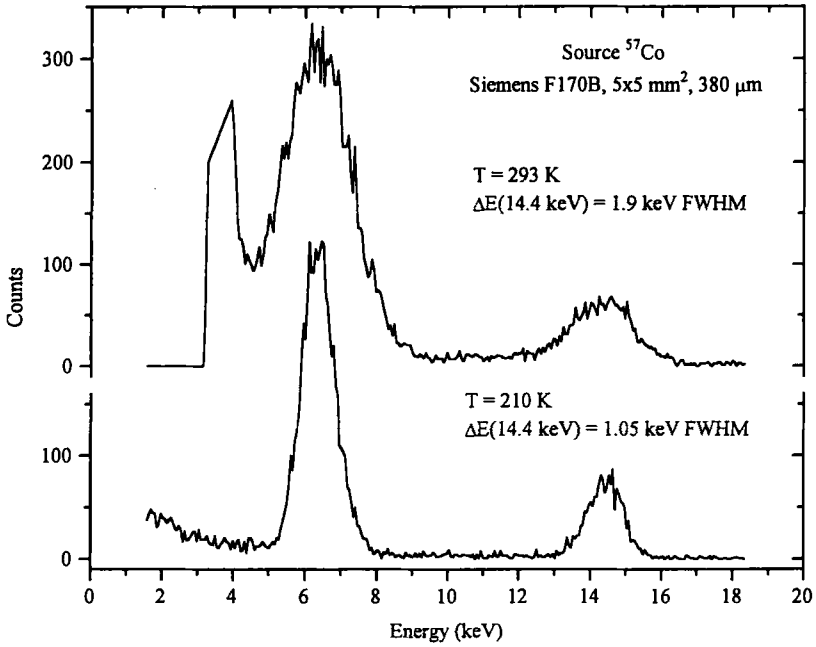


Fig. 3. Energy spectra of a $^{57}\text{Co}/\text{Rh}$ source with a $5 \times 5 \text{ mm}^2$ PIN diode of $380 \mu\text{m}$ thickness at two temperatures.

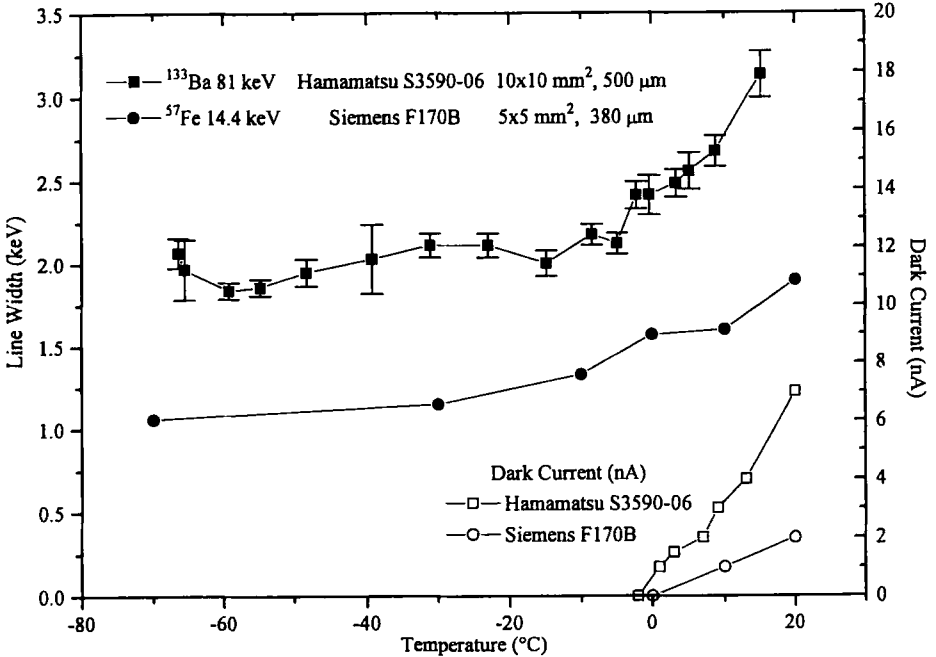


Fig. 4. Energy resolution and dark current of a $10 \times 10 \text{ mm}^2$ and a $5 \times 5 \text{ mm}^2$ PIN diode measured as a function of temperature.

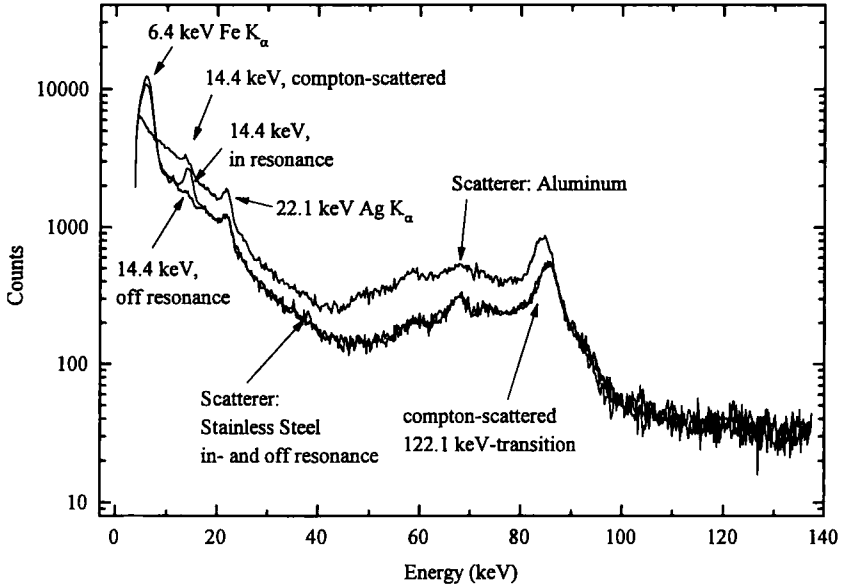


Fig. 5. Energy spectra of backscattered $^{57}\text{Co}/\text{Rh}$ radiation, measured with a $5 \times 5 \text{ mm}^2$ Si-PIN diode, thickness $380 \mu\text{m}$, using a prototype of the MIMOS spectrometer. Scatterers: 1 cm thick aluminum and stainless steel plates; for the case of SS, scattered spectra were measured in and off resonance. The recording time was the same for all three spectra.

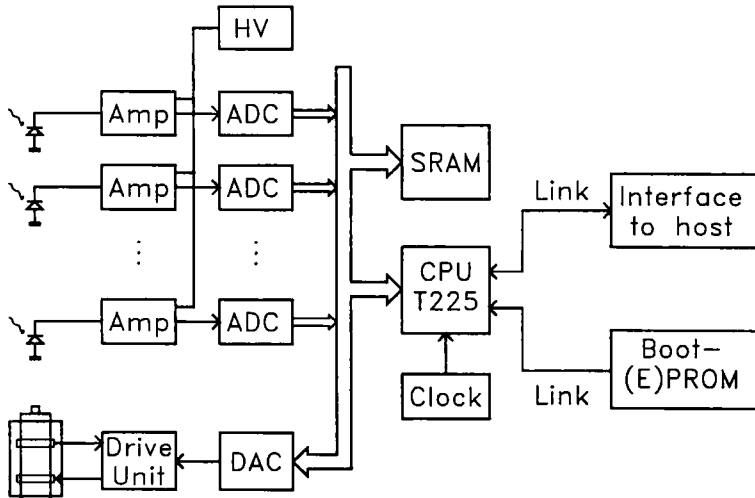


Fig. 6. Scheme of the electronic part of MIMOS. "Amp" consists of the preamplifier, connected to the PIN diode, and the Gauss amplifier. For a detailed description, see text.

The ADC conversion time has to be short for the rather high count rates expected. Also for this reason, the Gauss filter amplifiers provide bipolar output pulses allowing good resolution up to 10 kHz.

At least one channel will be used for high resolution X-ray fluorescence spectroscopy. This one could be most simply run under identical conditions as the other channels.

The seventh channel for velocity calibration of the MB drive has a simplified system with just one lower-level discriminator.

The 100 V dc voltage for the diodes is generated by a high-frequency cascade circuitry with a power consumption of less than 5 mW.

The operational control of the experiment and the data handling is done by a transputer which is suitable for fast real-time applications (fig. 6). The choice of this microprocessor was also dictated by the wide experience we have in using them in a transputer tree for the read out of a multiwire chamber for the Kaon spectrometer at GSI [40,41].

The main parts of the CPU module are a 16-bit transputer T225 running with 20 MHz clock frequency, a 64 Kbyte static RAM to hold the program and spectrum data, and some control logic contained in an ASIC (application specific integrated circuit). The control program is stored in a 128 Kbyte (E)EPROM and will be transferred to the RAM via a transputer link at power on time. The large (E)EPROM capacity allows storage of more than one copy of the control program in order to increase security against bit faults. Communication with the host computer of the rover will be done using a second transputer link or some other serial interface. All parts of the CPU module are realized in low-power CMOS technology.

The transputer generates the clock-driven analog reference signal for the drive using a 12-bit DAC. In the multiscaler mode, it provides the digital filtering of the 6.4 and 14.4 keV ADC signals. The selected events of the different detector channels are routed by the transputer to the actual velocity channel of the corresponding Mössbauer spectra. With about 25 Hz drive frequency and 512 channels per MB spectrum, all this has to be done in less than approximately 80 μ s.

In addition, measurements of temperature, vibrations, and energy spectra are controlled by the transputer.

3.4. FIRST EXPERIMENTAL RESULTS

To demonstrate the high MB efficiency, the velocity spectrum for SS is shown in fig. 7. The line is considerably broadened due to hyperfine field distributions. However, also an additional line broadening due to thickness effects has to be considered [23]. Its absolute value depends strongly on the sample properties and scattering angles. First experimental results using SS absorbers indicate only a small change in linewidth due to nonlinear resonant absorption. This is in reasonably good agreement with preliminary calculations.

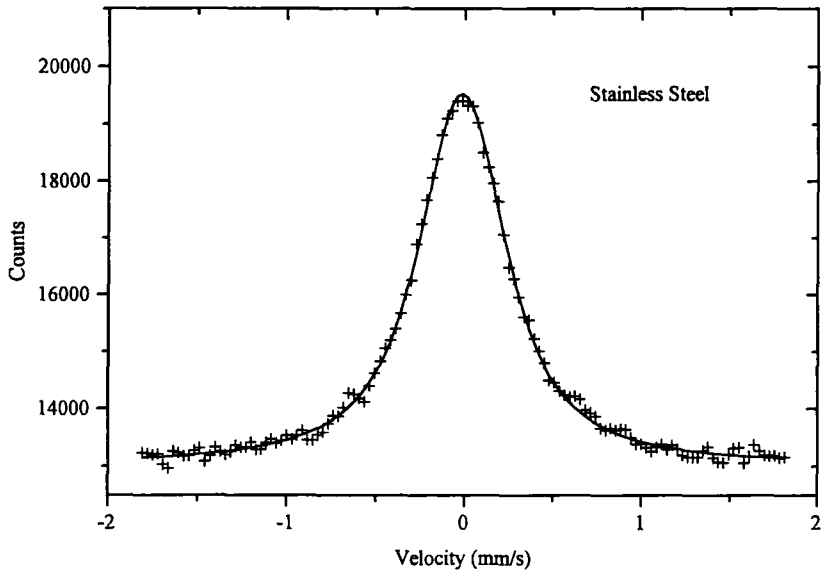


Fig. 7. MB backscattering spectrum at 14.4 keV from a stainless steel plate in MIMOS geometry.

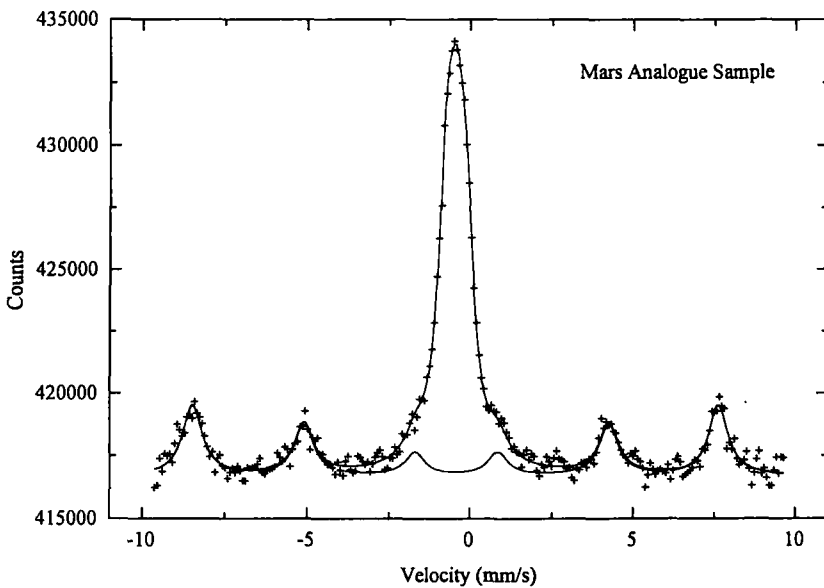


Fig. 8. MB spectrum of a Mars sample analogue [7], reflecting the elemental composition of the Martian soil, recorded with a only partially equipped prototype of the MIMOS spectrometer.

Assuming a dilution of the resonant part over a broader velocity domain, the decisive ratio of resonant to nonresonant absorption is reduced. This leads very quickly to a much stronger decrease of the relative line broadening. Also the penetration depths are increased and the intensities decreased. These statements also apply to the hyperfine split spectra expected from Mars samples. No additional broadening is to be expected.

Using a prototype of the setup shown in fig. 1, but not fully equipped, we have recorded MB spectra at 14.4 keV for a Mars sample analog [7]: 80% iron-rich clay (nontronite; SWa-1), 5% iron oxide ($\gamma\text{-Fe}_2\text{O}_3$), 10% MgSO_4 and $\frac{2}{3}\%$ of CaSO_4 , CaCO_3 and $\text{Fe}_2(\text{SO}_4)_3$, respectively (composition given in wt.%). The maximum emission angle of the 30 mCi $^{57}\text{Co/Cr}$ source was limited to 20° . Extrapolating to a fully equipped MIMOS setup, the spectrum given in fig. 8 can be measured with the same statistical quality in less than one hour. This result demonstrates the suitability for space research.

4. Summary and outlook

The construction of this MB system would not be feasible for our small group if all the components of the MB system had not been developed and used in different contexts in the past. The drive system, for instance, is part of the DCEMS Orange spectrometer [24,25,34]. Transputers were used in great quantity for a multiwire chamber at GSI and will be used for a PIN diode array with the front-end systems described above [35].

What about the future of Mössbauer Spectroscopy in Space?

By now, four years have passed since the first realistic proposals for a Mössbauer spectrometer were made [3, 13]. After joining the Mars'96 project about three years ago, we had the experience that the method of Mössbauer spectroscopy was not well known in the planetary science community. This is mainly due to the fact that up to this time, no space qualified MB spectrometer was available with existing technologies.

However, the situation has changed completely by now and MB spectroscopy is now widely accepted as a new tool for this field of science. Besides the Russian Mars'96 mission, in the European MARSNET proposal – a network of fixed stations on the surface of Mars – Mössbauer spectroscopy is also included. Recently, a proposal for a more powerful European Mars Rover was presented to ESA, also having an MB spectrometer on board. But MB spectroscopy is being considered not only for Mars. The ESA cornerstone mission ROSETTA, which is already decided upon, will go to a comet with an MB spectrometer included in the model payload of the lander module, descending to the surface of this interplanetary body.

In addition to the development of the instrument, a number of laboratories have started programs on so-called Mars Sample Analogues, which are not only

studied by the MB technique. Correlations of the MB results to magnetic properties, reflectance spectroscopic data, etc., are most important [6,7,26–33]. We believe that in this interdisciplinary field also others than space scientists will join, for instance, archaeologists studying the history of ancient potteries [43,44].

Similarly as in reflectance spectroscopy, the albedo for the MB radiation is important for the analysis of MB backscattering experiments. Because this is also important for the optimization of this instrument, we have started a program in this direction.

The knowledge gained from all these activities will play a decisive role when data are finally returned from Mars.

Acknowledgements

This experiment is performed in cooperation with IKI Space Research Institute, Moscow, the Mössbauer group at the University of Copenhagen, Denmark, and the Centre d'Etude Spatiale des Rayonnements, Toulouse, France. We are grateful to Professor H. Wänke, Dr. R. Rieder and W. Huth at the MPI für Kosmochemie, Mainz, for the possibility of performing experiments at their institute and for their friendly support. This work is supported by DARA, Bonn.

References

- [1] Mars-94/96, unmanned spacecraft mission to Mars (brief description), Jan. 1991, Space Research Inst., Vernadsky Inst. Geochemistry and Analytic Chemistry, USSR Academy of Sciences, Babakin Center, USSR.
- [2] Scientific results of the Viking Project, *J. Geophys. Res.* 82 (28) (1977).
- [3] J. Galazka-Friedman and J. Juchniewicz, Project Proposal, Space Research Center, Polish Academy of Sciences (February 1989).
- [4] D.G. Agresti, R.V. Morris, E.L. Wills, T.D. Shelfer, M.M. Pimperl, M. Shen, B.C. Clark and B.D. Ramsey, *Hyp. Int.* 72(1992)285.
- [5] J.M. Knudsen, *Hyp. Int.* 47(1989)3.
- [6] J.M. Knudsen, S. Mørup and J. Galazka-Friedman, *Hyp. Int.* 57(1990)2231.
- [7] J.M. Knudsen, M.B. Madsen, M. Olsen, L. Vistisen, C.B. Koch, S. Mørup, E. Kankeleit, G. Klingelhöfer, E.N. Evlanov, V.N. Khromov, L.M. Mukhin, O.F. Prilutskii, B. Zubkov, G.V. Smirnov and J. Juchniewicz, *Hyp. Int.* 68(1992)83.
- [8] J.M. Coey, S. Mørup, M.B. Madsen and J.M. Knudsen, *J. Geophys. Res.* 95 (B9) (1990) 14423.
- [9] G. Klingelhöfer and E. Kankeleit, Internal Proposal to Russian Space Agency IKI for an additional experiment using magnetic separation capabilities of a magnet array (1992).
- [10] Internal Report of the Centre National d'Etudes Spatiales (CNES), Toulouse, France, on the technical requirements on providing the planetary quarantine during conduction of the Mars 94/96 missions (April 1993).
- [11] E. Kankeleit, *Rev. Sci. Instr.* 35(1964)194.
- [12] E. Kankeleit, *Proc. Int. Conf. on Mössbauer Spectroscopy*, Vol. 2, Cracow, Poland (1975) p. 43.
- [13] R.V. Morris, D.G. Agresti, T.D. Shelfer and T.J. Wdowiak, *Lunar and Planet. Sci.* 20(1989)721.
- [14] T.D. Shelfer, M.M. Pimperl, D.G. Agresti, E.L. Wills and R.V. Morris, *Lunar and Planet. Sci.* 22(1991)1229.

- [15] J. Foh, P. Held, H. Jäger, E. Kankeleit, G. Klingelhöfer and U. Imkeller, *Ann. Geophys. Suppl.* 9(1991)C452.
- [16] E.N. Evlanov, L.M. Mukhin, O.F. Prilutski, G.V. Smirnov, J. Juchniewicz, E. Kankeleit, G. Klingelhöfer, J.M. Knudsen and C. d'Uston, *Lunar and Planet. Sci.* 22(1991)361.
- [17] E.N. Evlanov, V.A. Frolov, O.F. Prilutski, A.M. Rodin and G.V. Veselova, Internal Report, Space Research Institute (IKI), Moscow, Russia.
- [18] E.N. Evlanov, V.A. Frolov, O.F. Prilutski, A.M. Rodin, G.V. Veselova and G. Klingelhöfer, *Lunar and Planet. Sci.* 24(1993)459.
- [19] A.W. Gummer, *Nucl. Instr. Meth.* B34(1988)224.
- [20] P. Held, R. Teucher, G. Klingelhöfer, J. Foh, H. Jäger and E. Kankeleit, *Lunar and Planet. Sci.* 24(1993)633.
- [21] M.B. Madsen, J.M. Knudsen, L. Vistisen and R.B. Hargraves, *Lunar and Planet. Sci.* 24(1993)917.
- [22] J.M. Knudsen, private communication.
- [23] J. Lipka, M.N. Madsen, C. Bender Koch, M. Miglierini and L. Toth, these Proceedings, *Hyp. Int.*
- [24] B. Stahl, R. Gellert, O. Geiss, G. Klingelhöfer, G. Walter, R. Heitzmann and E. Kankeleit, to be submitted (in 1994).
- [25] G. Klingelhöfer, B. Stahl, U. Imkeller, R. Gellert, O. Geiss and E. Kankeleit, to be submitted (in 1994)
- [26] R.V. Morris, D.G. Agresti, H.V. Lauer, Jr., J.A. Newcomb, T.D. Shelfer and A.V. Murali, *J. Geophys. Res.* 94(1989)2760.
- [27] R.V. Morris and H.V. Lauer, Jr., *J. Geophys. Res.* 95(1990)5101.
- [28] J.L. Bishop, C.M. Pieters and R.G. Burns, *Lunar and Planet. Sci.* 24(1993)115.
- [29] J.L. Bishop, C.M. Pieters, S.F. Pratt and W. Patterson, *Lunar and Planet. Sci.* 24(1993)117.
- [30] J.L. Bishop, C.M. Pieters and R.G. Burns, *Geochim. Cosmochim. Acta* 57 (19), in press.
- [31] A. Banin, D.F. Blake and T. Benschlomo, *Lunar and Planet. Sci.* 22(1991)49.
- [32] A. Banin, B.C. Clark and H. Wänke, Surface chemistry and mineralogy, in: *Mars*, eds. H.H. Kieffer, B.M. Jakosky, C.W. Snyder and M.S. Matthew (The University of Arizona Press, Tucson-London, 1992).
- [33] J.F. Bell III, T.B. McCord and P.D. Owensby, *J. Geophys. Res.* 95(1990)14447.
- [34] B. Stahl, G. Klingelhöfer, H. Jäger, H. Keller, Th. Reitz and E. Kankeleit, *Hyp. Int.* 58(1990)2547.
- [35] S. Laubach, P. Schwalbach, M. Hartick, E. Kankeleit, G. Klingelhöfer and R. Sielemann, *Z. Phys.* B75(1989)173.
- [36] Ch. Weinheimer, M. Schrader, J. Bonn, Th. Loeken and H. Backe, *Nucl. Instr. Meth.* A311(1992)273.
- [37] T.E. Economou, J.S. Iwanczyk and R. Rieder, *Nucl. Instr. Meth.* A 322(1992)633.
- [38] D.G. Agresti, E.L. Wills, T.D. Shelfer, J.S. Iwanczyk, N. Dorri and R.V. Morris, *Lunar and Planet. Sci.* 21(1990)5.
- [39] O. Prilutskii, (IKI), Internal Report from Minsk (1990).
- [40] P. Baltes, J. Foh, H. Jäger, E. Kankeleit, Ch. Müntz, H. Oeschler, S. Sartorius, A. Wagner and the KaoS Collaboration, GSI Scientific Report (1990) p. 346.
- [41] P. Baltes, Diploma Thesis, Institute for Nuclear Physics, TH Darmstadt (1993).
- [42] G. Klingelhöfer, U. Imkeller, E. Kankeleit and B. Stahl, *Hyp. Int.* 71(1992)1445.
- [43] Y. Maniatis, A. Simopoulos and A. Kostikas, *J. Am. Ceramic Soc.* 66 (11) (1983) 773.
- [44] Y. Maniatis, A. Simopoulos, R.E. Jones, Ch. Karakalos, I.K. Whitbread, C.K. Williams II and A. Kostikas, *J. Field Archaeol.* 11(1984)205.
- [45] We acknowledge the support of the French Space Agency in supporting us for doing part of the tests with 100 g accelerating forces over a broad bandwidth.